American Journal of Pathology, Vol. 163, No. 3, September 2003

Nitration of Tau Protein Is Linked to Neurodegeneration in Tauopathies

Takashi Horiguchi,* Kunihiro Uryu,* Benoit I. Giasson,* Harry Ischiropoulos,† Richard LightFoot,† Christine Bellmann,‡ Christiane Richter-Landsberg,‡ Virginia M.-Y. Lee,* and John Q. Trojanowski*

From the Department of Pathology and Laboratory Medicine, Center for Neurodegenerative Disease Research, Institute on Aging, University of Pennsylvania School of Medicine, Philadelphia, Pennsylvania; the Department of Biochemistry and Biophysics,† Children's Hospital of Philadelphia, and University of Pennsylvania, Philadelphia, Pennsylvania; and the Department of Biology,‡ Molecular Neurobiology, University of Oldenburg, Oldenburg, Germany*

Oxidative and nitrative injury is implicated in the pathogenesis of Alzheimer's disease (AD) and Down syndrome (DS), but no direct evidence links this type of injury to the formation of neurofibrillary tau lesions. To address this, we generated a monoclonal antibody (mAb), n847, which recognizes nitrated tau and α-synuclein. n847 detected nitrated tau in the insoluble fraction of AD, corticobasal degeneration (CBD), and Pick's disease (PiD) brains by Western blots. Immunohistochemistry (IHC) showed that n847 labeled neurons in the hippocampus and neocortex of AD and DS brains. Double-label immunofluorescence with n847 and an anti-tau antibody revealed partial co-localization of tau and n847 positive tangles, while n847 immmunofluorescence and Thioflavin-S double-staining showed that a subset of n847-labeled neurons were Thioflavin-S-positive. In addition, immuno-electron microscopy revealed that tau-positive filaments in tangle-bearing neurons were also labeled by n847 and IHC of other tauopathies showed that some of glial and neuronal tau pathologies in CBD, progressive supranuclear palsy, PiD, and frontotemporal dementia with parkinsonism linked to chromosome 17 also were n847-positive. Finally, nitrated and Thioflavin-S-positive tau aggregates were generated in a oligodendrocytic cell line after treatment with peroxynitrite. Taken together, these findings imply that nitrative injury is directly linked to the formation of filamentous tau inclusions. *(Am J Pathol 2003, 163:1021–1031)*

Oxidative and nitrative injury has been implicated in the pathogenesis of neurodegenerative disorders including Alzheimer's disease (AD),[1–6] Down syndrome (DS),[7,8] amyotrophic lateral sclerosis,[9] Huntington's disease,[10] and various synucleopathies.[11,12] Oxidative injury occurs when the production of reactive species overwhelms the compensatory antioxidant capacity of cells. Reactive oxygen and nitrogen species are produced *in vivo* and may act synergistically to form nitrating agents that modify proteins as well as other biomolecules such as thiols, aldehydes, and lipids.[13,14] Specifically, tyrosine residues or free tyrosine can be modified by peroxynitrite, a compound generated by the reaction of superoxide anion and nitric oxide to generate 3-nitrotyrosine (3-NT). Anti-3-NT polyclonal antibodies revealed immunoreactive 3-NT in hallmark lesions of neurodegenerative diseases such as neurofibrillary tangles (NFTs) in AD[4,5,15] and Lewy bodies in Parkinson's disease (PD).[12,16–18]

Tau is an abundant microtubule-associated protein of the central nervous system that is primarily expressed in neurons, but also in glia at lower levels.[19–21] The functions of tau are to bind and stabilize microtubules in the polymerized state.[22,23] The discovery of multiple pathogenic tau gene mutations in many different families afflicted by frontotemporal dementia with parkinsonism linked to chromosome 17 (FTDP-17) showed unequivocally that tau abnormalities cause neurodegenerative disease.[24–26] Several lines of evidence suggest that abnormal phosphorylation as well as tau gene mutations impair the function of tau.[27–30] Indeed, abnormally phosphorylated tau is the major building block of the paired helical filaments (PHFs) in NFTs of AD and DS, and filamentous neuronal and glial tau inclusions are signature brain lesions of corticobasal degeneration (CBD), progressive supranuclear palsy (PSP), Pick's disease (PiD), and FTDP-17.[31]

Previously, we showed that α-synuclein (α-Syn) proteins in synucleinopathy lesions are specifically nitrated.[12] In contrast, it is unclear whether or not nitrative injury also is linked to the pathogenesis of tauopathy lesions. To address this question, we identified a monoclonal antibody (mAb), designated n847, which we pre-

Supported by National Institutes of Health grants AG14449 and AG17586.

Accepted for publication June 3, 2003.

V.M.-Y. L is the John H. Ware Third Chair of Alzheimer's Disease Research and J.Q.T. is the William Maul Measey-Truman G. Schnabel, Jr., M.D. Professor of Geriatric Medicine and Gerontology.

Address reprint requests to Dr. John Q. Trojanowski, Center for Neurodegenerative Disease Research, Department of Pathology and Laboratory Medicine, Hospital of The University of Pennsylvania/Maloney, Third Floor, Philadelphia, PA 19104-4283. E-mail: trojanow@mail.med.upenn.edu.

viously raised against nitrated forms of α-Syn, but which also preferentially recognizes nitrated tau as well as nitrated α-Syn. We show here that mAb n847 recognizes nitrated forms of tau protein in the brains of AD, CBD, and PiD patients by Western blots and by immuno-electron microscopy (immuno-EM). In light microscopic immunohistochemical (IHC) and fluorescence IHC (FIHC) analyses, we demonstrated variable distribution patterns of nitrated tau proteins in tauopathy lesions by comparing the localization of n847 immunoreactive (IR) profiles with those stained by anti-pan tau antibodies and/or Thioflavin-S (Thio-S). Finally, we showed that nitrated tau aggregates can be generated in an oligodendroglial cell line after peroxynitrite treatment.

Materials and Methods

Generation of n847

The n847 mAb was raised against recombinant human α-Syn (hα-Syn) protein nitrated *in vitro*.[32] Briefly, nitrated hα-Syn (100 μg) emulsified in Freund's complete adjuvant was injected subcutaneously in BALB/c mice, followed by a subcutaneous injection of 25 μg of nitrated hα-Syn emulsified in Freund's incomplete adjuvant on day 21 and an intravenous injection of 25 μg of nitrated hα-Syn in phosphate-buffered saline on day 48. On day 51, the spleen was removed and the lymphocytes were fused to myeloma cells (line Sp2/0-Ag14) using polyethylene glycol 1500.

Western Blotting

Proteins were resolved on slab gels by SDS-PAGE and electrophoretically transferred onto nitrocellulose membranes (Schleicher and Schuell, Keene, NH) in buffer containing 48 mmol/L Tris, 39 mmol/L glycine and 10% methanol. Membranes were blocked with a 5% solution of powdered milk dissolved in Tris buffered saline-Tween (50 mmol/L Tris, pH 7.6, 150 mmol/L NaCl, 0.1% Tween-20), incubated with primary antibodies followed with either a goat anti-mouse IgG horseradish peroxidase (HRP) conjugated antibody or a goat anti-rabbit HRP-conjugated antibody (Jackson Immunoresearch Laboratories, Inc., West Grove, PA) and visualized using enhanced chemiluminescence (NEN, Boston, MA) or by the peroxidase method with 3,3′-diaminobenzidine as the chromogen.

Antibody Characterization

The largest isoform of human tau (htau40) and hα-Syn proteins were expressed as recombinant proteins in *Escherichia coli* BL21 (DE3) RIL and purified as described.[26,33,34] Site-directed mutagenesis was used to substitute each of the four Tyr (Y) residues in hα-Syn to Phe (F) thereby yielding Y39F, Y125F, Y133F, and Y136F mutants as well as a quadruple mutant hα-Syn wherein all four Tyr residues were replaced with Phe[34] by using a Site-Directed Mutagenesis kit (QuikChange, La Jolla, CA). These recombinant proteins as well as RNase A, cytochrome c (cyto c), bovine superoxide dismutase-1 (SOD-1), and phospholipase A2 (PLA_2) were nitrated as described.[12,32] To determine the specificity of n847, 50 ng of each of the nitrated or unmodified proteins was loaded in individual lanes of 7.5% or 12% SDS-polyacrylamide gels, and n847 IR bands were identified by Western blot analysis as described above.

To test the specificity of the n847 antibody for 3-NT-modified tau proteins, Western blots were performed on these proteins following dithionite reduction. To do this, triplicate samples of tau in PHF fractions (PHF-tau) of AD cortex were subjected to SDS-PAGE and transfered to nitrocellulose membranes that were immersed in 0.5 mol/L dithionite (sodium hydrosulfite, Sigma, St. Louis, MO) in 0.1 mol/L NaOH for 15 minutes at room temperature, and then washed extensively in Tris-buffered saline (TBS). Before addition of dithionite, the NaOH buffer was purged of oxygen by bubbling N_2 into 50 ml of the solution for 15 minutes, and membranes were placed in a 50-ml screw-cap tube to exclude atmospheric O_2. One membrane was probed with n847, another one was probed with with an anti-tau mAb cocktail containing the T14 and T46 mAbs following reduction, and the third membrane was not subjected to denitration before being probed with n847, and all of the Western blots were developed as described above.

Biochemical Assessment of Tau Nitration in Diseased and Control Brain

Western blot analyses of tau proteins in the frontal cortex from the brains of AD ($n = 3$), CBD ($n = 1$), PiD ($n = 1$), and normal control cases ($n = 3$) were performed. PHF-tau protein fractions from each sample of cortex were prepared by sequential extraction as described.[30] Briefly, cortical gray matter (1 g) was dissociated with a Dounce homogenizer using 0.8 ml of high salt (HS) buffer (50 mmol/L Tris, 10 mmol/L, EGTA, 5 mmol/L $MnSO_4$, 0.75 mol/L NaCl, 0.02 mol/L NaF) and centrifuged at 100,000 × *g* for 25 minutes. The resulting pellets were re-extracted with 10 ml of PHF buffer (10 mmol/L Tris pH 7.6, 0.85 mol/L NaCl, 1 mmol/L EDTA, 20 mmol/L NaF, 10% sucrose). After centrifugation at 20,000 × *g* for 25 minutes, sarkosyl was added (final concentration, 1%) to the supernatant and incubated for 1 hour at room temperature. Then, the sample was centrifuged at 100,000 × *g* for 45 minutes and the resulting pellets were used as the PHF-tau fraction. Samples were resolved on 7.5% polyacrylamide gels, followed by Western blot analysis as described above, with n847, PHF-1, or combination of T14 and T46.

Immunohistochemical Analysis

Data on the brain samples used here in the IHC analyses are listed in Table 1. The brain regions examined included hippocampus, temporal and frontal cortex, as well as cerebellal cortex from the patients with AD, DS, and several tauopathies (ie, PiD, CBD, PSP, FTDP-17),

Table 1. Cases Studied

Disease	Number	Age		Sex	PMI**	
		Mean year	SD	(Male/Female)	Mean (hours)	SD
AD *possible	3	82	1	1/2	10.7	3.2
probable	6	79.7	7.7	3/3	10.9	5.2
definite	19	78.2	10.7	7/12	10.1	6.6
DS	5	58.2	14.4	4/1	18.0	12.3
CBD	3	67	6.9	2/1	12.8	5.8
PSP	3	81.7	0.6	2/1	3.5	1.8
PiD	3	71	3.6	2/1	8.5	5.8
FTDP-17	3	73	10.1	1/2	9.7	3.2
Normal control	9	65.4	19.1	5/4	15.9	8.5

*, Stages of AD are according to CERD criteria,[43] possible, probable, and definite correspond to I–II, III–IV, and V–VI in Braak and Braak's classification,[42] respectively. **, PMI, post-mortem interval.

AD, Alzheimer's disease; DS, Down syndrome; CBD, corticobasal degeneration; PSP, progressive suranuclear palsy; PiD, Pick disease; FTDP-17, frontotemporal demetia with parkinsonism linked to chromosome-17.

and controls with no degenerative pathologies. The brains were fixed in 70% ethanol in 150 mmol/L NaCl, pH 7.4, or in 10% neutral buffered formalin and processed for IHC analyses using n847 and a panel of antibodies to other neurodegeneration-related proteins (see Table 2 for details on this antibody panel) as described previously.[35,36] The antibody-probed slides were developed with avidin-biotin complex (ABC) method (Vectastain ABC Kit, Vector Laboratories, Burlingame, CA) using positive and negative controls as described.[35,36] Semiquantitative analysis of n847-IR CA1 neurons was conducted by examining eight photographs of the CA1 region of each section from each case using 20X lens and a Nikon-FXA microscope. Neurons with different n847 staining patterns were identified, counted, and statistically analyzed using analysis of variance.

To confirm that n847 labeling co-localized with filamentous tau-positive lesions in the tauopathies studied here, double-label FIHC analysis was performed as described above. Briefly, following overnight incubation of sections with a mixture of n847 and 17024, a polyclonal antibody to recombinant tau proteins, the sections were rinsed in buffer and incubated for 1 hour with a mixture of Texas Red-conjugated goat anti-mouse IgG (IgG) and FITC-conjugated goat anti-rabbit IgG, or Texas Red-conjugated goat anti-rabbit IgG (IgG) and FITC-conjugated goat anti-mouse IgG (Jackson ImmunoResearch Laboratories, West Grove, PA). After subsequent washes, the sections were cover-slipped with Vectashield-DAPI (4′, 6′-diamidino-2-phenylindole) mounting medium (Vector Laboratories, Burlingame, CA), and analyzed using a fluorescent microscope (Nikon-FXA) or a confocal microscope (Ti/Sapphire lasers: Coherent Mira 900-F lasers with Verdi pump and Bio-Rad, MRC 1024). In addition, we performed double-label experiments using n847 FIHC and Thio-S staining. Controls included adjacent sections individually stained with n847 or Thio-S. In the double-labeling experiments, Thio-S staining was performed after n847 immunofluorescence labeling, and in preliminary experiments, we found no differences in the order of Thio-S and n847 staining.

Immuno-Electron Microscopy

Hippocampus from the brains of patients with AD, CBD, and PiD were processed for single- or double-label preembedding immuno-EM with or without silver enhancement as described.[37] Double immuno-EM studies using the n847 mAb and the 17024 anti-tau rabbit polyclonal antibodies were performed as described with minor modifications.[38] Subsequently, the tissues were dehydrated by a graded series of ethanol as well as propylene oxide and embedded in EPON812. Ultra-thin sections were cut and examined under an electron microscope (JEOL, JEM-1010).

Cell Culture

To study the effects of nitration on the aggregation of tau, OLN-93 cells, a permanent oligodendroglial cell line derived from primary rat brain glial cultures,[39] were stably transfected with the Tau40 cDNA to express the longest human tau isoform as described.[40] A cell line stably

Table 2. Antibodies Used in this Study

Antibody	Type	Antigen recognized	Dilution used for		Reference or company
			WB	IHC	
n847	mouse mAb	nitrated-tau/-α-syn	1:500	1:2000	This study
17024	rabbit polyclonal	tau	—	1:2000	54
T14	mouse mAb	tau	1:500	1:3000	55
T46	mouse mAb	tau	1:500	1:1000	56
PHF-1	mouse mAb	phospholyrated tau	1:500	—	57
NT-3	rabbit polyclonal	3-nitrotyrosine	1:5000	1:50*	Upstate Biotechnology

*, Affinity purified.

expressing tau (OLN-Tau40) was established by subcloning for use in the studies described here. OLN-Tau40 cells were grown in DMEM supplemented with 10% fetal bovine serum (FBS), 2 mmol/L glutamine, 100 IU/ml penicillin, and 100 μg/ml streptomycin. Peroxynitrite (0.5 mmol/L) (Upstate Biotechnology, Charlottesville, VA) treatment was conducted on cells in DMEM/0.5% FBS for the indicated times, and cell lysates were prepared and subjected to immunoblot analysis and FIHC. For immunoblot analysis, monolayers of control and peroxynitrite-treated cells were washed with PBS twice, scraped off in sample buffer containing 1% SDS, and boiled for 10 minutes. Protein concentrations in the samples were determined according to published methods.[41] Total cellular extracts were separated by one-dimensional SDS-PAGE using 7.5% polyacrylamide gels followed by Western blot analysis with n847 and the 17024 anti-tau antibody as described above. For FIHC, cells were cultured for 2 days on poly-L-lysine-coated glass cover-slips (2×10^4 cells per 35-mm dish) in DMEM/0.5%FBS, and treated with 0.5 mmol/L peroxynitrite. After 24 hours, cells were fixed with 3% paraformaldehyde and permeabilized with 0.1% Triton for 15 minutes. The cover-slips were washed three times and incubated for 1 hour with mAb n847 (1:500) and rabbit polyclonal anti-tau (17024) antiserum (1:500) for single- and double-label FIHC as described above, and nuclei were stained by including 4,6-diamino-2-phenylindole (DAPI) (1 μg/ml) to the mounting medium, while Thio-S staining was combined with FIHC as described above.

Results

Characterization of n847

To examine the possible nitration of tau in pathological lesions of AD, DS, and tauopathies, previously raised mAbs generated to nitrated hα-Syn were screened for cross-reactivity with nitrated tau. Several mAbs were identified that recognized the nitrated recombinant longest human tau isoform (htau40), and we characterized these further using Western blot analysis with nitrated and unmodified species of tau and various other proteins. We found that one mAb, ie, n847, preferentially recognized nitrated htau40 in addition to hα-Syn and dimers with an apparent molecular mass (Mr) of ~35 kd. However, it did not recognize non-nitrated tau or other nitrated proteins used as controls such as RNaseA, cyto c, SOD-1, or PLA_2 (Figure 1A). These results indicated that n847 preferentially recognizes nitrated tau and nitrated hα-Syn, and the properties of n847 are therefore distinct from the pan anti-nitrated-tyrosine residue-specific polyclonal antibody anti-3-NT which recognizes 3-NT residues regardless of the protein context.[12]

Western blot analysis revealed that n847 recognizes PHF-tau proteins in sarkosyl-insoluble PHF-tau fractions prepared from the gray matter of AD, CBD, and PiD frontal cortex. Specifically, n847 strongly detected three distinct bands in all three AD brains and two distinct bands in CBD and PiD brains, which were of Mr 50 to 70 kd, but none of these bands were detected in sarkosyl-insoluble fractions isolated from control brains. Notably these bands also were detected by a combination of anti-tau mAbs (T14/T46) as well as the PHF-tau-specific mAb known as PHF-1 (Figure 1B). These results also were confirmed by striping and re-probing immunoblots that were first probed with n847, and in these experiments, the blots were probed with either PHF-1 or T14/T46. In addition, n847 detected no bands in the HS-soluble fraction of any of the brains tested (data not shown). Finally, additional Western blot analyses revealed a higher specificity of the n847 mAb for AD PHF-tau than that seen with the anti-3-NT antibody, which recognized tau proteins as well as many other protein bands in PHF-tau fractions (Figure 1C). To further demonstrate that m847 mAb indeed recognize nitrated tau, PHF-tau protein from AD brains were denitrated and probed with n847 in Western blots. Reduced staining of denitrated tau was observed using n847 mAb but not with nitration-independent mAbs T14/T46 in the denitrated PHF-tau samples (Figure 1D).

To test the specificity of n847 for protein modified by 3-NT, WT, and single or quadruple Tyr to Phe, point mutants of recombinant hα-Syn were exposed to peroxynitrite and subjected to Western blot analysis. The blots probed with the LB509 mAb to non-modified hα-Syn labeled monomeric, dimeric, and trimeric forms of WT and single hα-Syn mutants (Figure 1E, left). The blots probed with the n847 mAb detected peroxynitrite-treated hα-Syn containing at least one Tyr residue, but n847 did not detect hα-Syn with quadruple Tyr to Phe substitutions (Figure 1E, right).

Nitrated Tau in NFTs of AD and DS Brains

In IHC studies of hippocampus from AD patients, where there is abundant tau pathology (eg, Braak and Braak stage III-IV,[42] CERAD criteria - probable AD[43]), n847 labeled numerous neurons, especially in CA1, although the intracellular distribution of n847 IR varied considerably (see Figure 2). These patterns can be classified into four types: type 1 neurons with faint n847 IR products located in the cell body (Figure 2b); type 2 neurons with the IR products filling perikarya and dendrites (Figure 2c); type 3 neurons containing NFTs with the IR products partially filling neuronal perikarya and/or dendrites (Figure 2d); and type 4 neurons containing NFTs with the IR products that occupied limited regions of perikarya and dendrites (Figure 2e). These four types of n847 IR patterns also were seen in CA1 regions of the DS brain. In AD cases with Braak and Braak stage III-IV NFT pathology,[42] most neurons showed type 2 or 3 staining, but in AD cases with a Braak and Braak stage V-VI and CERAD criteria-definite AD,[43] type 4 was the major staining pattern (see histogram and accompanying table in Figure 2). These n847 IR patterns did not seem to be affected by age, sex, and PMI, but the higher the Braak and Braak stage, the greater the number of type 3 and 4 n847-stained neurons. In contrast to AD and DS, the CA1 region of young normal cases showed almost exclusively the type 1 staining pattern (Figure

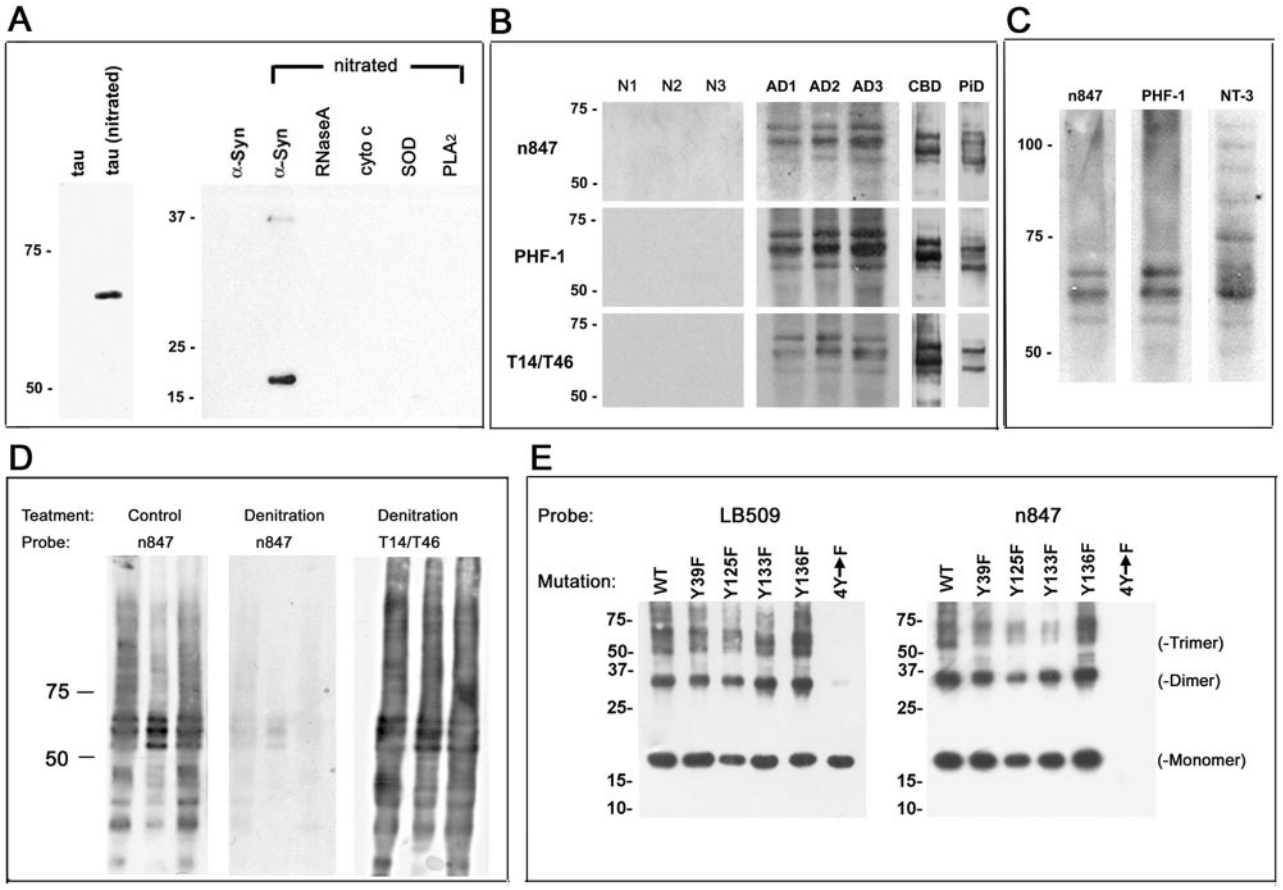

Figure 1. Characterization of the n847 mAb. **A:** The specificity of n847 for nitrated tau. Fifty ng of each protein shown were loaded in corresponding lanes of 7.5% (**left**) or 12% (**right**) SDS-polyacrylamide gels, separated by electrophoresis, and transferred to nitrocellulose membranes that were probed with n847 and developed by enhanced chemiluminescence (ECL). **B:** The n847 mAb recognized sarkosyl-insoluble nitrated tau protein in AD (AD1-AD3), CBD, and PiD but not in normal (N1-N3) brains. PHF-tau fractions from frontal cortical gray matter of each brain were isolated biochemically and analyzed by Western blot using n847, T14/T46, and PHF-1 antibodies as described in the text. **C:** Similar PHF-tau bands are recognized by n847 and the 3-NT antibodies, but 3-NT also recognizes other nitrated proteins in AD brains. Shown in (**C**) is a PHF-tau fraction isolated from AD brain (as in **B**) analyzed by Western blot with n847, PHF-1, and anti-3-NT. **D:** The n847 mAb specifically recognizes nitrated tau proteins. Shown in (**D**) are native (control lanes) and denitrated PHF-tau proteins from AD brains examined by Western blot illustrating the reduced staining with n847 in the denitrated AD PHF-tau sample compared to the control sample. Denitration did not affect PHF-tau staining by the nitration independent anti-tau mAbs T14/T46. **E:** Western blots demonstrate the specificity of mAb n847 for 3-NT modified hα-Syn proteins. Wild-type and Tyr (Y) to Phe (F) point mutants of recombinant hα-Syn were exposed to peroxynitrite as described in the text, and 25 ng of each protein were loaded in separate lanes of 12% SDS polyacrylamide gels for Western blot analysis with mAb LB509 to native hα-Syn and the n847 mAb. Note that LB509 shows that equal amounts of hα-Syn proteins were loaded in each lane, but n847 preferentially recognizes peroxynitrite-treated α-Syn containing at least one Tyr residue, but not the Tyr-deficient hα-Syn protein (4Y→F). The hα-Syn trimers and dimers (identified on the **right**) probably reflect dityrosine cross-linking.

2g), while aged normal control brains showed predominantly type 1 staining with much smaller numbers of type 2, 3, and 4 neurons. As shown in the histogram and table in Figure 2, in early stages of AD pathology development (Braak and Braak I-II), the majority (61.7%) was categorized as type 2 cells and in more advanced stages (Braak and Braak V-VI) the predominant cell staining pattern (46.46%) was type 4 cell (Figure 2C). A decrease of type 1 (from 25.11% to 11.10%) and 2 cells (61.70% to 11.76%) and an increase of type 4 (2.39% to 46.46%) cells were noted as the stage shifted from the early to advanced stage.

Apart from CA1 region, the CA2–3 regions of the hippocampus from the AD and DS brains also showed all four types of staining patterns. Specifically, as the Braak and Braak stages increased, the number of neurons with type 2, 3, and 4 staining patterns extended from CA1 to the CA2–3 regions. These types of staining patterns were not observed in normal controls in these regions.

Furthermore, CA1–4 neurons expressing both PHF-1 IR and n847 IR products were categorized as type 2, 3, or 4 cells, and n847 IR always co-localized, at least partially, with PHF-1 IR products (data not shown). However, n847 IHC studies of the cerebellum of AD and normal cases revealed very light type 1 n847 staining in Purkinje neurons (Figure 2h), and these cells do not accumulate NFTs.

Comparison of Non-Nitrated Tau and Nitrated Tau Localization

To further examine the relationship between n847 IR products and NFTs in pyramidal neurons, we focused on CA1 neurons, and performed double-label immunofluorescence with n847 mAb, and 17024 (pan-tau) polyclonal antibodies on a number of AD cases using conventional fluorescence and confocal microscopy. In AD cases, CA1 neurons with all of the four n847 staining patterns described above were

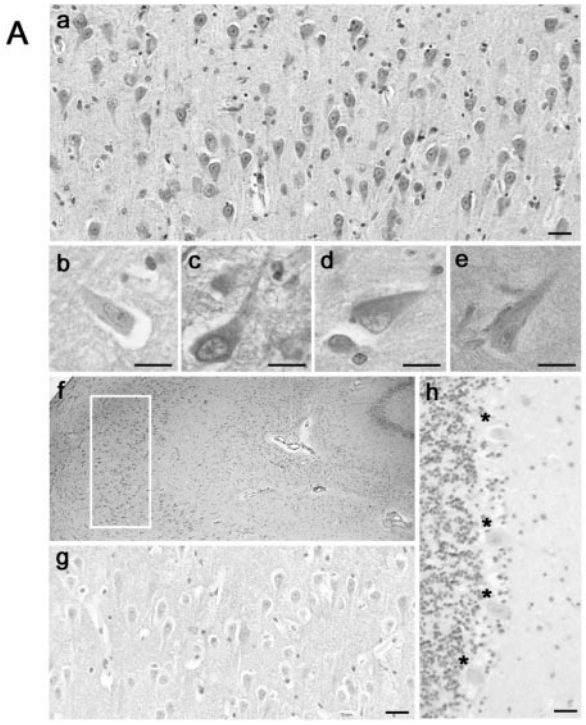

C

	Type 1	Type 2	Type 3	Type 4
I-II	25.11± 7.81	61.70 ±18.01	10.81 ±6.14	2.39 ± 4.12
III-VI	19.78 ± 6.08	22.16 ± 2.71	30.62 ± 1.22	27.45 ± 10.01
V-VI	11.10 ± 2.93	11.76 ± 9.63	30.69 ± 5.03	46.46 ± 17.03

Figure 2. IHC analyses of the AD hippocampus with mAb n847. **A:** N847 IR in the CA1 region of AD patients (Braak and Braak stage III-IV,[43] CERAD criteria - probable AD[44]). Low-power views of CA1 (**a** corresponds to the boxed region of **f**) showing diverse n847 IR in pyramidal neurons. Four types of n847 IR in neuron are shown (ie, types 1, 2, 3, and 4 in **b, c, d**, and **e**, respectively, as described in the text). As the Braak stage[42] advanced, the number of type 3 and 4 neurons in the CA1 region increased but only type 1 neurons (**b**) were observed in young normal control brains (**g**, low-power view), while n847 IR was very weak in cerebellum of AD and normal brain (**h**, Braak stage V-VI in AD). *, indicates Purkinje cells. **Bars**, 10 μm. **B** and **C:** Semi-quantitative analysis shows a shift of n847 IR with progression of AD. The signature of early stage (I-II) of AD was predominance of type 2 n847 IR, but this type of staining diminished as the Braak stage advanced. On the other hand, types 3 and 4 n847 IR were insignificant in stage I-II, but increased significantly at later Braak stages while type 4 n847 IR predominated at Braak stage V-VI.

all 17024-positive except the type 1-stained neurons, although co-localization of n847 and 17024 staining varied (see Figure 3Aa–c and confocal inset). Type 2 cells showed prominent 17024 IR and n847 IR (Figure 3Aa). Type 3 had intensive 17024 staining and modest n847 positivity (Figure 3Ab). Type 4 exhibited intense 17024 staining and scant n847 IR (Figure 3Ac).

Interrelationship between Nitrated Tau and Thio-S Staining

Next, we used Thio-S staining, a dye that binds NFTs and other amyloids,[44] to compare the distribution of nitrated-tau and Thio-S-labeled NFTs. To do this, we performed double-label FIHC with n847 mAb and 17024 antibodies on one section, and Thio-S staining plus 17024 FIHC on an adjacent section. These studies showed a unique relationship between the n847 and Thio-S staining (see Figure 3, B and C). By comparing this set of sections, examination of the relationship between the localization of n847 IR products and Thio-S staining in 17024-positive neurons in these cells was performed. As expected, only a subset of 17024 and n847 IR-positive neurons possessed Thio-S-positive staining (Figure 3B, arrow and Figure 3Ca). These n847 positive neurons were either Thio-S-negative (Figure 3Ba, arrow and Figure 3Ca), or Thio-S-positive (Figure 3Ba, arrowhead and Figure 3Cb and c). Some 17024-postitive neurons with intense and uniform Thio-S failed to show n847 staining (Figure 3Cd).

Nitration of Tau in Diverse Tauopathies

Next, we examined nitrated-tau in neurodegenerative lesions of various tauopathies, including CBD, PSP, PiD, and FTDP-17. The globose NFT-like structures in the pons of PSP (Figure 4Aa) and in the substantia nigra of CBD (Figure 4Ab), and ballooned neurons in the midfrontal cortex of CBD (Figure 4Ac) were positively stained, respectively. Pick body-like inclusions in the entorhinal cortex and hippocampus of PiD (Figure 4Ad) and FTDP-17 (Figure 4Ae) cases were also stained. Labeling of small numbers of glial tau inclusions (coiled bodies) also was evident in these tauopathies (Figure 4Af), but no cells in the cerebellum showed n847 staining (data not shown).

To confirm that n847 labels nitrated tau in these tauopathy lesions, double-label immunofluorescence analysis with n847 and 17024 was performed, which showed that n847 labeled globose NFTs (Figure 4Ba), Pick bodies (Figure 4Bb), coiled bodies (Figure 4Bc), and ballooned neurons (Figure 4Bd) that co-localized partially with 17024-positive tau IR, and this was confirmed by confocal microscopy (Figure 4Be and f).

Immuno-EM Analysis of Nitration on NFTs

To further confirm the presence of nitratively altered tau in NFTs, we performed double and single immuno-EM analyses with n847 and 17024 in hippocampal sections from the brains of patients with AD, CBD, and PiD. In AD cases, immuno-EM, with n847 alone demonstrated IR products associated with filamentous structures in NFT of CA1 pyramidal neurons (Figure 4Ca), and similar nSyn 847 staining was seen in Pick bodies and CBD tangles (data not shown). Finally, Figure 4Cb shows representative images of individual tau filaments that are double-

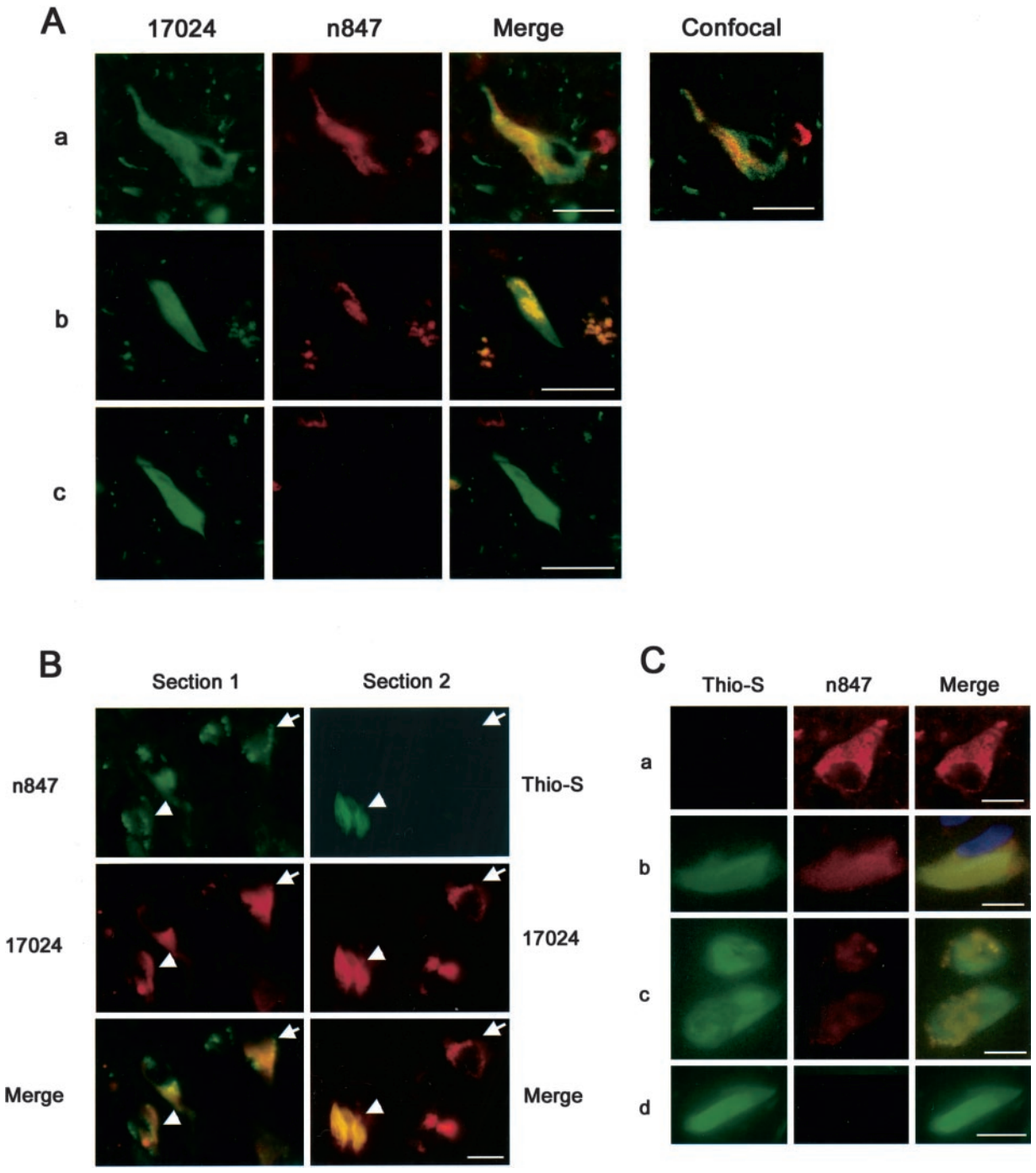

Figure 3. Double-labeling of AD NFTs at various stages with n847 and 17024/Thio-S. **A:** The n847 IR co-localizes with 17024 IR NFTs. Shown in **a**, **b**, and **c** of **A** are representative images of types 2, 3 and 4 n847 IR cells, respectively. Co-localization of staining is seen in the merged images and by confocal microscopy. **Bars**, 10 μm. **B:** The n847 IR is evident in pre-tangles. To identify neurons containing nitrated NFTs, adjacent sections were labeled with combination of n847 and 17024 (section 1) or Thio-S and 17024 (section 2) as described in the text. Thio-S-positive and -negative neurons are indicated by **arrowhead** and **arrow**, respectively. **C:** Double-label studies of NFTs by n847 and Thio-S. Four representative labeling patterns of Thio-S are shown: (**a**) none; (**b**) uniformly moderate; (**c**) mixed intense and moderate; (**d**) uniformly intense. Note that the n847 IR decreases as Thio-S labeling increases. **Bars**, 10 μm.

labeled with both n847 (10-nm gold particles) and 17024 (5-nm gold particles) by immuno-EM.

Nitration of Transfected Tau in Cultured Cells

To directly investigate the association between nitration of tau and inclusion formation, OLN-Tau40 cells were subjected to peroxynitrite treatment (0.5 mmol/L) and analyzed by combination of FIHC and Thio-S staining methods 24 hours after treatment. The distribution of total tau was demonstrated with the anti-tau antibody 17024 (Figure 5 Aa, d, g, and j). Exposure to peroxynitrite resulted in Thio-S staining (Figure 5Ae) as well as nitrated tau IR (Figure 5k) within tau IR regions, and this staining pattern was not seen in

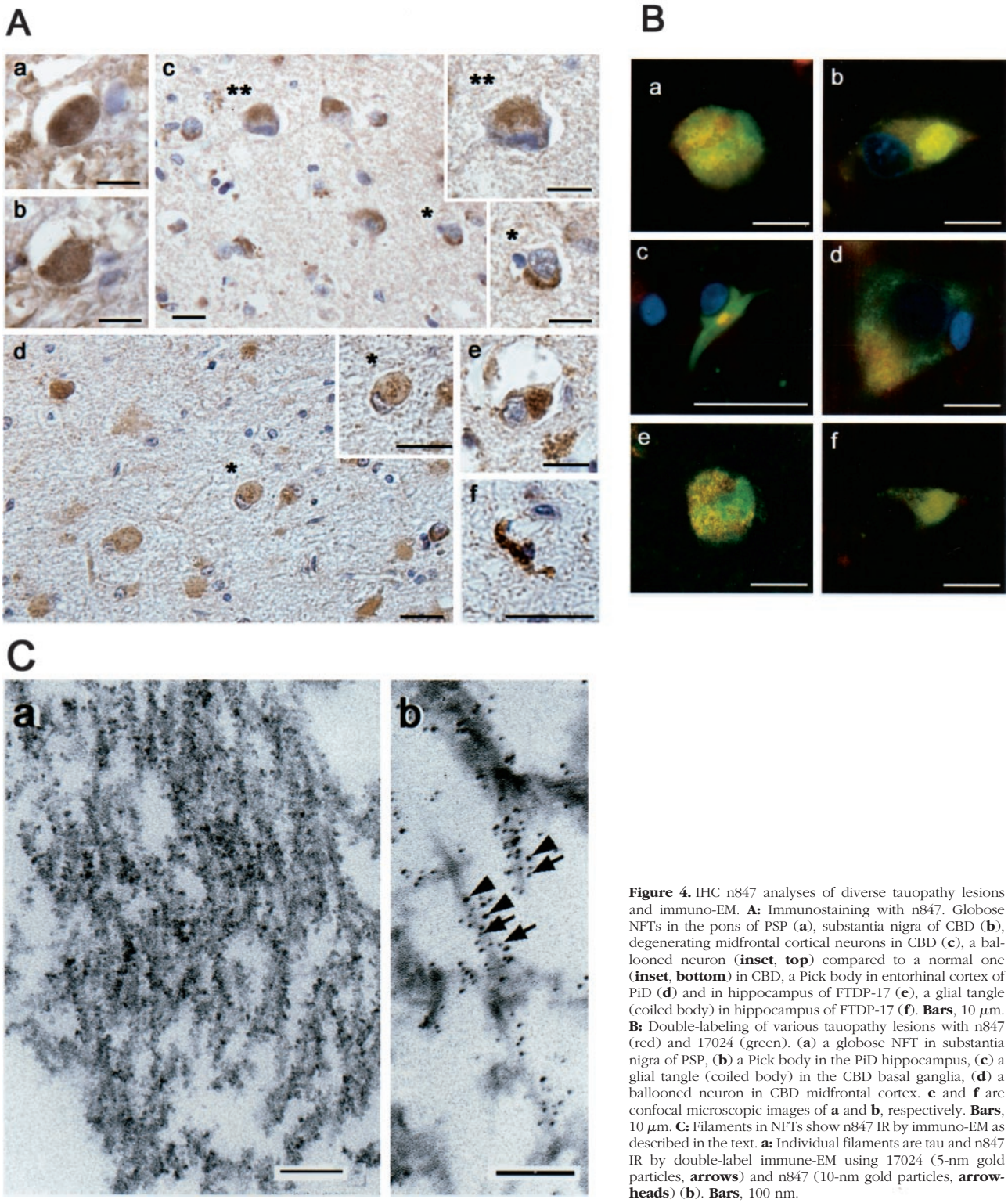

Figure 4. IHC n847 analyses of diverse tauopathy lesions and immuno-EM. **A:** Immunostaining with n847. Globose NFTs in the pons of PSP (**a**), substantia nigra of CBD (**b**), degenerating midfrontal cortical neurons in CBD (**c**), a ballooned neuron (**inset**, **top**) compared to a normal one (**inset**, **bottom**) in CBD, a Pick body in entorhinal cortex of PiD (**d**) and in hippocampus of FTDP-17 (**e**), a glial tangle (coiled body) in hippocampus of FTDP-17 (**f**). **Bars**, 10 μm. **B:** Double-labeling of various tauopathy lesions with n847 (red) and 17024 (green). (**a**) a globose NFT in substantia nigra of PSP, (**b**) a Pick body in the PiD hippocampus, (**c**) a glial tangle (coiled body) in the CBD basal ganglia, (**d**) a ballooned neuron in CBD midfrontal cortex. **e** and **f** are confocal microscopic images of **a** and **b**, respectively. **Bars**, 10 μm. **C:** Filaments in NFTs show n847 IR by immuno-EM as described in the text. **a:** Individual filaments are tau and n847 IR by double-label immune-EM using 17024 (5-nm gold particles, **arrows**) and n847 (10-nm gold particles, **arrowheads**) (**b**). **Bars**, 100 nm.

untreated control cells (Figure 5Ab and h). As shown in Figure 5B, biochemical studies confirmed the presence of nitrated tau in lysates of OLN-Tau40 cells treated with peroxynitrite (0.5 mmol/L) but not in untreated control lysates.

Discussion

The present study demonstrated that n847, a novel mAb which recognizes a nitrated form of tau protein, links nitrative modifications of tau in cytoplasmic cellular inclu-

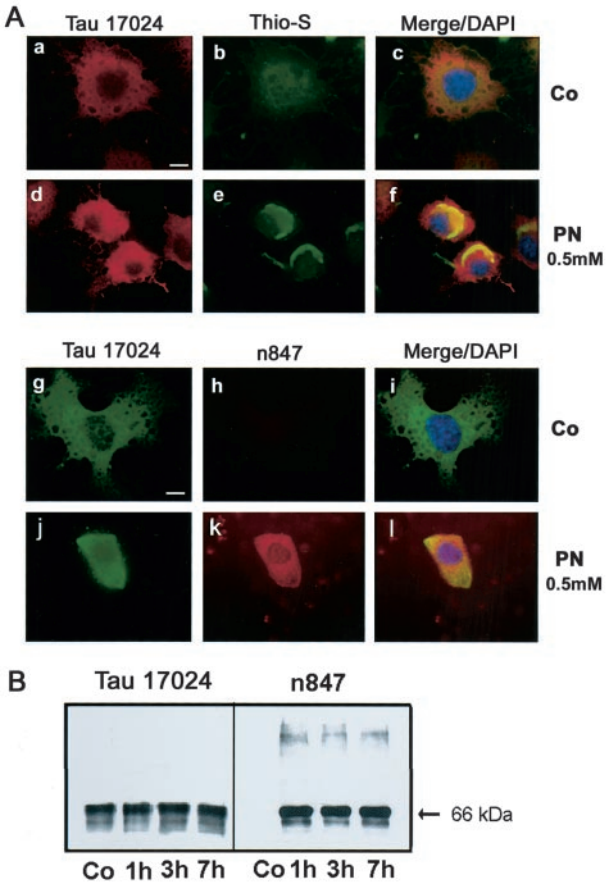

Figure 5. IHC and Western blot studies of cultured oligodendroglia. OLN-Tau40 cells were peroxynitrite treated (0.5 mmol/L) and analyzed 24 hours after treatment. **A:** Control (Co) or peroxynitrite (PN)-treated cells were studied by FIHC with the 17024 polyclonal antibody (**a**, **d**, **g**, **j**), followed by Thio-S (**b** and **e**) or n847 staining (**h** and **k**) and nuclei of cells (**c**, **f**, **i**, **l**) were counterstained by DAPI. Images are shown in single (**a**, **b**, **d**, **e**, **g**, **h**, **j**, **k**) or merged (**c**, **f**, **i**, **l**) views. **Bar**, 10 μm. **B:** Tau is nitrated in cultured OLN-Tau40 cells treated with peroxynitrite. Shown are Western blots of cell lysates from untreated control (Co) or peroxynitrite-treated OLN-Tau40 cells at 1, 3, and 7 hours post-nitration as described in the text. Note that n847 IR bands co-migrate with tau IR bands labeled by 17024, but in addition, higher molecular weight n847 IR bands are seen that are tau negative which may represent nitratively cross-linked species of tau that may have lost tau IR due to nitrative damage.

sions to mechanisms of disease in AD and several tauopathies, including CBD, PiD, PSP, and FTDP-17. In addition, the data presented here are consistent with the notion that nitrative damage to tau may be a pathological process that occurs dynamically at several steps in the sequence of events leading to the formation of glial and neuronal filamentous tau inclusions in selected regions of the diseased brain.

By comparing the staining patterns of n847 with that of PHF-1, 17024, and Thio-S, we showed that nitrated forms of tau detected by n847 co-localize with abnormal tau aggregates in a subset of pathological inclusions. Single-label studies with n847 were complemented by double-label studies with this mAb and anti-tau antisera as well as with anti-PHF-tau antibodies and Thio-S staining. Previous studies using anti-3-NT antibodies to detect 3-NT IR in NFTs in AD brains did not allow detection of specific nitrated species of tau in neurodegenerative disease lesions[4,5,15] as was possible here with the novel n847 mAb. Furthermore, nitrated tau was detected in PHF-fractions of AD, CBD, and PiD brain, but not in HS-soluble fractions. Thus, taken together, these results suggest that nitrative damage to tau may be involved in mechanisms leading to the formation of filamentous tau inclusions.

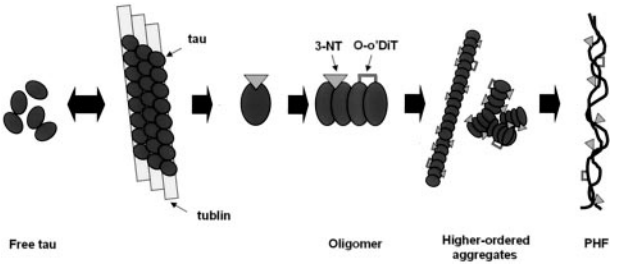

Figure 6. Schematic model of the possible role of nitrative/oxidative modifications in the formation of PHF. Under normal conditions, tau (**ovals**) is in equilibrium between a free and a microtubule-bound (**rectangular bars**) pool, where tau stabilizes microtubules. Nitrative damage of tau may reduce its affinity for microtubules resulting in unbound nitrated (**triangles**) tau, which may serve as a nidus for oligomer formation, but nitration also may enhance tau fibrillization. This polymerization process can lead to the formation of complex aggregates of PHFs. o-o' Dityrosine cross-linking (**brackets**) that occurs concomitantly with nitration[32] could also contribute to the stabilization of polymers.

The present study provides direct evidence of nitrative modification of tau protein during tau inclusion formation in AD and in various tauopathies thereby linking oxidative/nitrative damage to tau in mechanisms of AD and diverse tauopathies. Consistent with data showing heterogeneity of tau lesions in different tauopathies,[31] the presence of nitratively damaged tau protein in various tauopathies also was heterogeneous. Moreover, our analyses of the hippocampus from the brains of patients with AD suggests that the incorporation of nitrated/oxidized tau into NFTs is a step-wise or temporally sequential process involving four or more stages in the evolution of this pathology. However, the appearance of nitrated tau in NFTs appears to occur predominantly before the maturation of tau inclusions, since n847 immunoreactivity was stronger in tau inclusions that are weakly or not stained with Thio-S. The reasons for this are not clear at this time, but could reflect denitration of 3-NT residue enzymatically, destabilization of nitrated tau in the inclusions that form in AD and different tauopathies, or epitope masking by conformational alterations or by chemical modifications such as ubiquitination as tangles mature or undergo further pathological processing.

At the molecular level, as demonstrated in schematic model in Figure 6, it is plausible that nitration of tau could inhibit microtubule binding similar to the effects of phosphorylation.[22,45,46] Accumulation of free tau could lead to a critical threshold level that will promote dimerization/oligomerization leading to aggregation and the formation of largely polymers and, eventually, pathological inclusions. During this putative series of events, nitrative modification of tau may occur at one or several steps in this process with diverse consequences. For example, nitration could promote a conformation change in tau that may promote fibril assembly. Furthermore, o-o' dityrosine cross-linking that occurs concomitantly with nitration[34] may also

stabilize polymers at several stages of filament maturation. Other types of post-translation modifications resulting from oxidation damage have also been shown in NFTs[2,47–52] and these may also contribute to promote the formation of pathological inclusions. However, further studies are needed to test this hypothetical scenario including changes in gene expression that may underlie it.[53]

Acknowledgments

We thank the Biochemical Imaging Core Facility of the University of Pennsylvania for assistance with confocal and electron microscopy. Furthermore, we thank members of Center for Neurodegenerative Disease Research for their constructive supports. We also express our appreciation to the families of the many patients whose generosity made these studies possible.

References

1. Markesbery WR, Carney JM: Oxidative alterations in Alzheimer's disease. Brain Pathol 1999, 9:133–146
2. Takeda A, Smith MA, Avila J, Nunomura A, Siedlak SL, Zhu X, Perry G, Sayre LM: In Alzheimer's disease, heme oxygenase is coincident with Alz50, an epitope of tau induced by 4-hydroxy-2-nonenal modification. J Neurochem 2000, 75:1234–1241
3. Pratico D, Lee VMY, Trojanowski JQ, Rokach J, FitzGerald GA: Increased F2-isoprostanes in Alzheimer's disease: evidence for enhanced lipid peroxidation in vivo. EMBO J 1998, 12:1777–1783
4. Smith MA, Richey Harris PL, Sayre LM, Beckman JS, Perry G: Widespread peroxynitrite-mediated damage in Alzheimer's disease. J Neurosci 1997, 17:2653–2657
5. Hensley K, Maidt ML, Yu Z, Sang H, Markesbery WR, Floyd RA: Electrochemical analysis of protein nitrotyrosine and dityrosine in the Alzheimer brain indicates region-specific accumulation. J Neurosci 1998, 18:8126–8132
6. Lyras L, Cairns NJ, Jenner A, Jenner P, Halliwell B: An assessment of oxidative damage to proteins, lipids, and DNA in brain from patients with Alzheimer's disease. J Neurochem 1997, 68:2061–2069
7. Jovanovic SV, Clements D, MacLeod K: Biomarkers of oxidative stress are significantly elevated in Down syndrome. Free Radic Biol Med 1998, 25:1044–1048
8. Hayn M, Kremser K, Singewald N, Cairns N, Nemethova M, Lubec B, Lubec G: Evidence against the involvement of reactive oxygen species in the pathogenesis of neuronal death in Down's syndrome and Alzheimer's disease. Life Sci 1996, 59:537–544
9. Cookson MR, Shaw PJ: Oxidative stress and motor neurone disease. Brain Pathol 1999, 9:165–186
10. Browne SE, Ferrante RJ, Beal MF: Oxidative stress in Huntington's disease. Brain Pathol 1999, 9:147–163
11. Jenner P, Olanow CW: Understanding cell death in Parkinson's disease. Ann Neurol 1998, 44:S72–S84
12. Giasson BI, Duda JE, Murray IV, Chen Q, Souza JM, Hurtig HI, Ischiropoulos H, Trojanowski JQ, Lee VMY: Oxidative damage linked to neurodegeneration by selective α-synuclein nitration in synucleinopathy lesions. Science 2000, 290:985–989
13. O'Donnell VB, Eiserich JP, Chumley PH, Jablonsky MJ, Krishna NR, Kirk M, Barnes S, Darley-Usmar VM, Freeman BA: Nitration of unsaturated fatty acids by nitric oxide-derived reactive nitrogen species peroxynitrite, nitrous acid, nitrogen dioxide, and nitronium ion. Chem Res Toxicol 1999, 12:83–92
14. White CR, Patel RP, Darley-Usmar V: Nitric oxide donor generation from reactions of peroxynitrite. Methods Enzymol 1999, 301:288–298
15. Good PF, Werner P, Hsu A, Olanow CW, Perl DP: Evidence of neuronal oxidative damage in Alzheimer's disease. Am J Pathol 1996, 149:21–28
16. Good PF, Hsu A, Werner P, Perl DP, Olanow CW: Protein nitration in Parkinson's disease. J Neuropathol Exp Neurol 1998, 57:338–342
17. Gomez-Tortosa E, Gonzalo I, Newell K, Yebenes G, Vonsattel P, Hyman BT: Patterns of protein nitration in dementia with Lewy bodies and striatonigral degeneration. Acta Neuropathol (Berl) 2002, 103: 495–500
18. Duda JE, Giasson BI, Chen Q, Gur TL, Hurtig HI, Stern MB, Gollomp SM, Ischiropoulos H, Lee VMY, Trojanowski JQ: Widespread nitration of pathological inclusions in neurodegenerative synucleinopathies. Am J Pathol 2000, 157:1439–1445
19. Cleveland DW, Hwo SY, Kirschner MW: Purification of tau, a microtubule-associated protein that induces assembly of microtubules from purified tubulin. J Mol Biol 1977, 116:207–225
20. Binder LI, Frankfurter A, Rebhun LI: The distribution of tau in the mammalian central nervous system. J Cell Biol 1985, 101:1371–1378
21. Couchie D, Mavilia C, Georgieff IS, Liem RK, Shelanski ML, Nunez J: Primary structure of high molecular weight tau present in the peripheral nervous system. Proc Natl Acad Sci USA 1992, 89:4378–4381
22. Drechsel DN, Hyman AA, Cobb MH, Kirschner MW: Modulation of the dynamic instability of tubulin assembly by the microtubule-associated protein tau. Mol Biol Cell 1992, 3:1141–1154
23. Weingarten MD, Lockwood AH, Hwo SY, Kirschner MW: A protein factor essential for microtubule assembly. Proc Natl Acad Sci USA 1975, 72:1858–1862
24. Poorkaj P, Bird TD, Wijsman E, Nemens E, Garruto RM, Anderson L, Andreadis A, Wiederholt WC, Raskind M, Schellenberg GD: Tau is a candidate gene for chromosome 17 frontotemporal dementia. Ann Neurol 1998, 43:815–825
25. Hutton M, Lendon CL, Rizzu P, Baker M, Froelich S, Houlden H, Pickering-Brown S, Chakraverty S, Isaacs A, Grover A, Hackett J, Adamson J, Lincoln S, Dickson D, Davies P, Petersen RC, Stevens M, de Graaff E, Wauters E, van Baren J, Hillebrand M, Joosse M, Kwon JM, Nowotny P, Heutink P: Association of missense and 5′-splice-site mutations in tau with the inherited dementia FTDP-17. Nature 1998, 393:702–705
26. Hong M, Zhukareva V, Vogelsberg-Ragaglia V, Wszolek Z, Reed L, Miller BI, Geschwind DH, Bird TD, McKeel D, Goate A, Morris JC, Wilhelmsen KC, Schellenberg GD, Trojanowski JQ, Lee VMY: Mutation-specific functional impairments in distinct tau isoforms of hereditary FTDP-17. Science 1998, 282:1914–1917
27. Bramblett GT, Goedert M, Jakes R, Merrick SE, Trojanowski JQ, Lee VMY: Abnormal tau phosphorylation at Ser396 in Alzheimer's disease recapitulates development and contributes to reduced microtubule binding. Neuron 1993, 10:1089–1099
28. Goedert M, Spillantini MG, Jakes R, Rutherford D, Crowther RA: Multiple isoforms of human microtubule-associated protein tau: sequences and localization in neurofibrillary tangles of Alzheimer's disease. Neuron 1989, 3:519–526
29. Spillantini MG, Murrell JR, Goedert M, Farlow MR, Klug A, Ghetti B: Mutation in the tau gene in familial multiple system tauopathy with presenile dementia. Proc Natl Acad Sci USA 1998, 95:7737–7741
30. Lee VMY, Balin BJ, Otvos Jr L, Trojanowski JQ: A68: a major subunit of paired helical filaments and derivatized forms of normal tau. Science 1991, 251:675–678
31. Forman MS, Lee VMY, Trojanowski JQ: New insights into genetic and molecular mechanisms of brain degeneration in tauopathies. J Chem Neuroanat 2000, 20:225–244
32. Souza JM, Giasson BI, Chen Q, Lee VMY, Ischiropoulos H: Dityrosine cross-linking promotes formation of stable α-synuclein polymers: implication of nitrative and oxidative stress in the pathogenesis of neurodegenerative synucleinopathies. J Biol Chem 2000, 275:18344–18349
33. Norris EH, Giasson BI, Ischiropoulos H, Lee VMY: Effects of oxidative and nitrative challenges on α-synuclein fibrillogenesis involve distinct mechanisms of protein modifications. J Biol Chem 2003, 278:27230–27240
34. Giasson BI, Murray IV, Trojanowski JQ, Lee VMY: A hydrophobic stretch of 12 amino acid residues in the middle of α-synuclein is essential for filament assembly. J Biol Chem 2001, 276:2380–2386
35. Murai H, Pierce JE, Raghupathi R, Smith DH, Saatman KE, Trojanowski JQ, Lee VMY, Loring JF, Eckman C, Younkin S, McIntosh TK: Twofold overexpression of human β-amyloid precursor proteins in transgenic mice does not affect the neuromotor, cognitive, or neurodegenerative sequelae following experimental brain injury. J Comp Neurol 1998, 392:428–438
36. Nakagawa Y, Nakamura M, McIntosh TK, Rodriguez A, Berlin JA,

Smith DH, Saatman KE, Raghupathi R, Clemens J, Saido TC, Schmidt ML, Lee VMY, Trojanowski JQ: Traumatic brain injury in young, amyloid-β peptide overexpressing transgenic mice induces marked ipsilateral hippocampal atrophy and diminished Aβ deposition during aging. J Comp Neurol 1999, 411:390–398

37. Galvin JE, Uryu K, Lee VMY, Trojanowski JQ: Axon pathology in Parkinson's disease and Lewy body dementia hippocampus contains α-, β-, and γ-synuclein. Proc Natl Acad Sci USA 1999, 96:13450–13455
38. Smith RM, Jarret L: Electron microscopc immunocytochemical approaches to the localization of ligands, receptors, transducers, and transporters. Handbook of Endocrine Research Techniques. Edited by de Pablo F. San Diego, Academic Press, 1993, pp 227–264
39. Richter-Landsberg C, Heinrich M: OLN-93: a new permanent oligodendroglia cell line derived from primary rat brain glial cultures. J Neurosci Res 1996, 45:161–173
40. Vogelsberg-Ragaglia V, Bruce J, Richter-Landsberg C, Zhang B, Hong M, Trojanowski JQ, Lee VMY: Distinct FTDP-17 missense mutations in tau produce tau aggregates and other pathological phenotypes in transfected CHO cells. Mol Biol Cell 2000, 11:4093–4104
41. Neuhoff V, Philipp K, Zimmer HG, Mesecke S: A simple, versatile, sensitive and volume-independent method for quantitative protein determination which is independent of other external influences. Hoppe Seylers Z Physiol Chem 1979, 360:1657–1670
42. Braak H, Braak E: Neuropathological staging of Alzheimer-related changes. Acta Neuropathol (Berl) 1991, 82:239–259
43. Mirra SS, Heyman A, McKeel D, Sumi SM, Crain BJ, Brownlee LM, Vogel FS, Hughes JP, van Belle G, Berg L: The Consortium to Establish a Registry for Alzheimer's Disease (CERAD). Part II. Standardization of the neuropathologic assessment of Alzheimer's disease Neurology 1991, 41:479–486
44. Sun A, Nguyen XV, Bing G: Comparative analysis of an improved thioflavin-s stain, Gallyas silver stain, and immunohistochemistry for neurofibrillary tangle demonstration on the same sections. J Histochem Cytochem 2002, 50:463–472
45. Lindwall G, Cole RD: Phosphorylation affects the ability of tau protein to promote microtubule assembly. J Biol Chem 1984, 259:5301–5305
46. Gustke N, Steiner B, Mandelkow EM, Biernat J, Meyer HE, Goedert M, Mandelkow E: The Alzheimer-like phosphorylation of tau protein reduces microtubule binding and involves Ser-Pro and Thr-Pro motifs. FEBS Lett 1992, 307:199–205
47. Sasaki N, Fukatsu R, Tsuzuki K, Hayashi Y, Yoshida T, Fujii N, Koike T, Wakayama I, Yanagihara R, Garruto R, Amano N, Makita Z: Advanced glycation end products in Alzheimer's disease and other neurodegenerative diseases. Am J Pathol 1998, 153:1149–1155
48. Nunomura A, Perry G, Pappolla MA, Wade R, Hirai K, Chiba S, Smith MA: RNA oxidation is a prominent feature of vulnerable neurons in Alzheimer's disease. J Neurosci 1999, 19:1959–1964
49. Smith MA, Rottkamp CA, Nunomura A, Raina AK, Perry G: Oxidative stress in Alzheimer's disease. Biochim Biophys Acta 2000, 1502: 139–144
50. Perry G, Nunomura A, Hirai K, Takeda A, Aliev G, Smith MA: Oxidative damage in Alzheimer's disease: the metabolic dimension. Int J Dev Neurosci 2000, 18:417–421
51. Smith MA, Taneda S, Richey PL, Miyata S, Yan SD, Stern D, Sayre LM, Monnier VM, Perry G: Advanced Maillard reaction end products are associated with Alzheimer disease pathology. Proc Natl Acad Sci USA 1994, 91:5710–5714
52. Ledesma MD, Bonay P, Colaco C, Avila J: Analysis of microtubule-associated protein tau glycation in paired helical filaments. J Biol Chem 1994, 269:21614–21619
53. Ginsberg SD, Hemby SE, Lee VMY, Eberwine JH, Trojanowski JQ: Expression profile of transcripts in Alzheimer's disease tangle-bearing CA1 neurons. Ann Neurol 2000, 48:77–87
54. Ishihara T, Hong M, Zhang B, Nakagawa Y, Lee MK, Trojanowski JQ, Lee VMY: Age-dependent emergence and progression of a tauopathy in transgenic mice overexpressing the shortest human tau isoform. Neuron 1999, 24:751–762
55. Kosik KS, Orecchio LD, Binder L, Trojanowski JQ, Lee VMY, Lee G: Epitopes that span the tau molecule are shared with paired helical filaments. Neuron 1988, 1:817–825
56. Mawal-Dewan M, Henley J, Van de Voorde A, Trojanowski JQ, Lee VMY: The phosphorylation state of tau in the developing rat brain is regulated by phosphoprotein phosphatases. J Biol Chem 1994, 269: 30981–30987
57. Greenberg SG, Davies P, Schein JD, Binder LI: Hydrofluoric acid-treated tau_{PHF} proteins display the same biochemical properties as normal tau. J Biol Chem 1992, 267:564–569